

## Magnetic studies of Ta doping in $\text{Pr}_{1.5}\text{Ce}_{0.5}\text{Sr}_2\text{Cu}_2\text{NbO}_{10}$

M. Bennaïmias

*Department of Applied Science, University of California at Davis, Livermore, California 94550  
and Lawrence Livermore National Laboratory, Livermore, California 94550*

H. B. Radousky

*Department of Physics, University of California at Davis, Davis, California 95616  
and Lawrence Livermore National Laboratory, Livermore, California 94550*

C. M. Buford and A. B. Kebede

*Department of Physics, North Carolina Agricultural and Technical State University, Greensboro, North Carolina 27411*

M. McIntyre, T. J. Goodwin, and R. N. Shelton

*Department of Physics, University of California at Davis, Davis, California 95616*

(Received 14 June 1995; revised manuscript received 14 September 1995)

The  $\text{Pr}_{1.5}\text{Ce}_{0.5}\text{Sr}_2\text{Cu}_2\text{Nb}_{1-x}\text{Ta}_x\text{O}_{10}$  ( $0 \leq x \leq 1$ ) compounds display an in-plane weak ferromagnetic component similar to that observed in the  $\text{Nd}_2\text{CuO}_4$ -type  $T'$  structure. Zero-field-cooled and field-cooled magnetization spectra indicate that the magnetic peak, previously ascribed by neutron diffraction in the  $\text{Pr}_{1.5}\text{Ce}_{0.5}\text{Sr}_2\text{Cu}_2\text{NbO}_{10}$  system as originating from an interlayer Cu spin reorientation, shifts towards lower temperature as the content of Ta increases. In addition, the effective Pr ion moment obtained by Curie-Weiss fits to the magnetization data taken at fields sufficiently high to saturate the weak ferromagnetic component indicate that the long-range antiferromagnetic ordering of the Pr ions in these compounds ( $\sim 2.8\mu_B$ ) is not affected by the substitution of Ta in for Nb. The nature of the complex magnetic behavior of these compounds originates from a thermal competition between magnetocrystalline anisotropy and magnetic exchange interactions.

### I. INTRODUCTION

The interplay between Cu magnetism and high-temperature superconductivity in several layered rare-earth cuprate systems continues to be a topic of importance.<sup>1</sup> The motivation for this effort stems from observations of antiferromagnetic (AF) ordering of the Cu atoms in nonsuperconducting compounds possessing the  $\text{RBa}_2\text{Cu}_3\text{O}_{7-\delta}$  structure,<sup>2</sup> the  $\text{La}_2\text{CuO}_4$   $T$  phase structure,<sup>3</sup> and the  $\text{Nd}_2\text{CuO}_4$   $T'$  phase structure.<sup>4,5</sup> The Cu moments in these materials tend to exhibit strong two-dimensional (2D) magnetic correlations that exist up to very high temperatures. Any long-range 3D magnetic correlations that can exist at low temperatures typically disappear above room temperature. Several of the rare-earth cuprates and nickelates possessing the  $T$  and  $T'$  crystal structures have been shown to possess an additional weak ferromagnetic component within the AF domain of the Cu or Ni magnetic sublattice.

The weak ferromagnetic component in these compounds is believed to arise as a result of an antisymmetric exchange coupling of the Dzyaloshinsky-Moriya (DM) type between neighboring Cu or Ni moments induced by a local distortion that breaks the tetragonal symmetry of the  $\text{CuO}_2$  planes.<sup>6-8</sup> Due to this DM interaction, the Cu or Ni moments are slightly canted in the AF state, giving rise to the weak ferromagnetic component from each  $\text{CuO}_2$  or  $\text{NiO}_2$  plane which polarizes the rare-earth magnetic sublattice. In the sense of a mean-field approximation this polarization can be thought of as an internal magnetic field,  $H_i$ , generated by the canted

moments, acting on the rare-earth ions.

The weak ferromagnetism in these materials has been shown to have a strong dependence on their magnetothermal history.<sup>9</sup> Furthermore, the magnitudes of the weak ferromagnetic components have been shown to strongly depend on sample preparation techniques, indicating that the weak ferromagnetic properties are very sensitive to the presence of lattice defects—either structural distortions, oxygen disorder, or variations in the oxygen stoichiometry. In addition, studies have shown that doping of Ce or Th into compounds with the  $T'$  phase has the effect of depressing the weak ferromagnetism behavior of the  $\text{CuO}_2$  planes.<sup>10</sup> The findings from these studies suggest that the suppression of the weak ferromagnetic component is manifested by a lowering of the temperature at which the Cu moments order.

Similar weak ferromagnetic behavior have been recently reported in  $\text{Pr}_{1.5}\text{Ce}_{0.5}\text{Sr}_2\text{Cu}_2\text{MO}_{10}$  ( $M = \text{Nb}$  or  $\text{Ta}$ ) electrically insulating compounds.<sup>11</sup> As shown in Fig. 1, the layered crystallographic structure of these compounds is a composite of the  $\text{Pr}_2\text{CuO}_4$   $T'$  and  $\text{PrBa}_2\text{Cu}_3\text{O}_{7-\delta}$  crystal structures with substitution of  $\text{NbO}_2$  or  $\text{TaO}_2$  planes for the  $\text{CuO}$  chains, a fluorite structured  $(\text{Pr}_{1.5}\text{Ce}_{0.5})\text{O}_2$  middle layer replacing the single ion rare-earth layer, and strontium atoms substituted in for the barium atoms. The length of the unit cell is doubled along the  $c$  direction due to a glide plane introduced by the  $(\text{Pr}_{1.5}\text{Ce}_{0.5})\text{O}_2$  layer. The weak ferromagnetic component in these compounds is evidenced by the presence of irreversibility, a remnant magnetization, and magnetic hysteresis that develops below 130 K. Neutron diffraction measurements<sup>12</sup> have indicated that a noncollinear component in the AF ordering of the Cu moments, suggestive of a DM interaction,

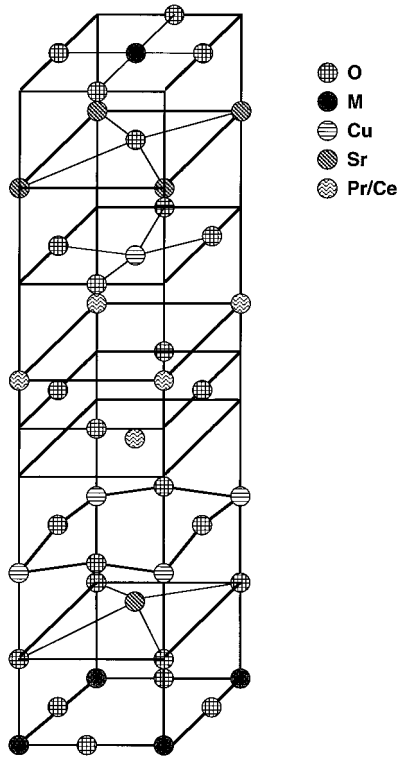


FIG. 1. Half of the  $R$ -Ce-Sr-Cu-Nb-O  $T^*$  phase crystallographic unit cell. Oxygens in the Nb, Sr, and Cu layers are designated as O(1) or O(5), O(4), and O(2) or O(3), respectively, while O(6) denotes the oxygens between the fluorite layers.

occurs below this temperature in the  $\text{Pr}_{1.5}\text{Ce}_{0.5}\text{Sr}_2\text{Cu}_2\text{NbO}_{10}$  insulator. The exact nature of the local structural distortion promoting the activation of the DM interaction is not presently known. Initial results<sup>11</sup> from zero-field-cooled and field-cooled magnetization profiles show that two magnetic ordering peaks ( $\sim 13$  K,  $\sim 56$  K) are observed in the  $\text{Pr}_{1.5}\text{Ce}_{0.5}\text{Sr}_2\text{Cu}_2\text{NbO}_{10}$  system but only a single peak ( $\sim 20$  K) is observed in the  $\text{Pr}_{1.5}\text{Ce}_{0.5}\text{Sr}_2\text{Cu}_2\text{TaO}_{10}$  system. The higher-temperature magnetic ordering peak, seen in the magnetization spectra for the  $\text{Pr}_{1.5}\text{Ce}_{0.5}\text{Sr}_2\text{Cu}_2\text{NbO}_{10}$  compound, has been previously ascribed by neutron diffraction measurements<sup>12</sup> to arise from an interlayer spin reorientation of the Cu moments.

In this paper, we report on the magnetic characteristics of a series of  $\text{Pr}_{1.5}\text{Ce}_{0.5}\text{Sr}_2\text{Cu}_2\text{Nb}_{1-x}\text{Ta}_x\text{O}_{10}$  ( $x=0.00, 0.25, 0.5, 0.6, 0.75, 1.00$ ) compounds. A lowering of the temperature at which the Cu spin reorientation occurs in these materials as a function of increasing Ta concentration is reported. The nature of the complex magnetic behavior of these compounds is ascribed to a thermal competition between magnetocrystalline anisotropy and magnetic exchange interactions.

## II. EXPERIMENTAL DETAILS

Polycrystalline samples of  $\text{Pr}_{1.5}\text{Ce}_{0.5}\text{Sr}_2\text{Cu}_2\text{Nb}_{1-x}\text{Ta}_x\text{O}_{10}$  ( $x=0.00, 0.25, 0.5, 0.6, 0.75, 1.00$ ) used in this study were synthesized through conventional solid-state reaction methods. Stoichiometric amounts of high purity (99.99% or better)  $\text{CeO}_2$ ,  $\text{Nd}_2\text{O}_3$ ,  $\text{Sm}_2\text{O}_3$ ,  $\text{Pr}_6\text{O}_{11}$ ,  $\text{SrCO}_3$ ,  $\text{CuO}$ ,  $\text{Nb}_2\text{O}_5$ , and  $\text{Ta}_2\text{O}_5$  dried powders were appropriately weighed, mixed together, and pressed into 3/8 inch pellets. The finished pellets

were placed in alumina crucibles and sintered at 1120 °C for 80 h in a slightly pressurized (approximately 30 kPa) oxygen atmosphere and then allowed to furnace cool to room temperature. Samples were then reground a second time, pressed again into pellets, and the firing process repeated. Powder x-ray-diffraction data (Siemens D-500 x-ray diffractometer) were taken on each of the samples that were used in this investigation in order to validate that these samples had the expected solid solution stoichiometry and not comprised of a double phase material. More detailed results of the x-ray-diffraction analysis performed on these types of compounds have been described elsewhere.<sup>13</sup>

The magnetization spectra were all taken on a commercially available Quantum Design rf superconducting quantum interference device (SQUID) magnetometer. Zero-field-cooled and field-cooled dc magnetization profiles over the temperature range 6–100 K were obtained for each compound for magnetic fields ranging from 10 to 5000 Oe. In addition, hysteresis data were measured for each compound in 5 K increments between 10 and 80 K and 50 K increments between 100 and 200 K over a magnetic-field excursion of  $\pm 50$  kOe. The data presented in this study were not corrected for demagnetizing factors since all the samples used were paramagnetic insulators ( $\chi_d \ll 1$ ) and therefore the correction was deemed to be negligible.

## III. EXPERIMENTAL RESULTS

Several zero-field-cooled and field-cooled magnetic spectra for these compounds were obtained for a broad range of applied magnetic-field strengths. The results of a compilation of one such data set for the samples used in this study, under the influence of an externally applied field of 500 Oe, are shown in Fig. 2. As can be readily seen from this figure, the zero-field-cooled magnetic behavior of the  $\text{Pr}_{1.5}\text{Ce}_{0.5}\text{Sr}_2\text{Cu}_2\text{NbO}_{10}$  sample (upper left) exhibits two magnetic transitions while only one ordering peak seems to be apparent in the magnetic spectra for the  $\text{Pr}_{1.5}\text{Ce}_{0.5}\text{Sr}_2\text{Cu}_2\text{TaO}_{10}$  sample (lower right). As one looks at each of the graphs depicted in Fig. 2 from the different samples, the magnetic peak at the higher temperature, that has been previously associated to a Cu spin reorientation and is here identified by the upward pointing arrows, shifts downward from around 56 K in the  $\text{Pr}_{1.5}\text{Ce}_{0.5}\text{Sr}_2\text{Cu}_2\text{NbO}_{10}$  compound to about 19 K in the  $\text{Pr}_{1.5}\text{Ce}_{0.5}\text{Sr}_2\text{Cu}_2\text{TaO}_{10}$  compound. Notably, two magnetic peaks are easily discernible in all of these graphs except for the one corresponding to the  $\text{Pr}_{1.5}\text{Ce}_{0.5}\text{Sr}_2\text{Cu}_2\text{TaO}_{10}$  compound. In order to determine the temperature at which the Cu moments would reorient in the  $\text{Pr}_{1.5}\text{Ce}_{0.5}\text{Sr}_2\text{Cu}_2\text{TaO}_{10}$  sample a Curie-Weiss analysis of the data for  $T > T_N + 10$  K was performed. Similar analysis were performed on the other samples and were found to be in excellent agreement with the values that were directly determined from the graphs shown in Fig. 2. In addition, Fig. 2 reveals that all of the samples displayed irreversible behavior characteristic of the weak ferromagnetism in these compounds. The irreversibility temperature, i.e., the temperature at which the zero-field-cooled and field-cooled magnetization data begin to deviate from one another, identified by the

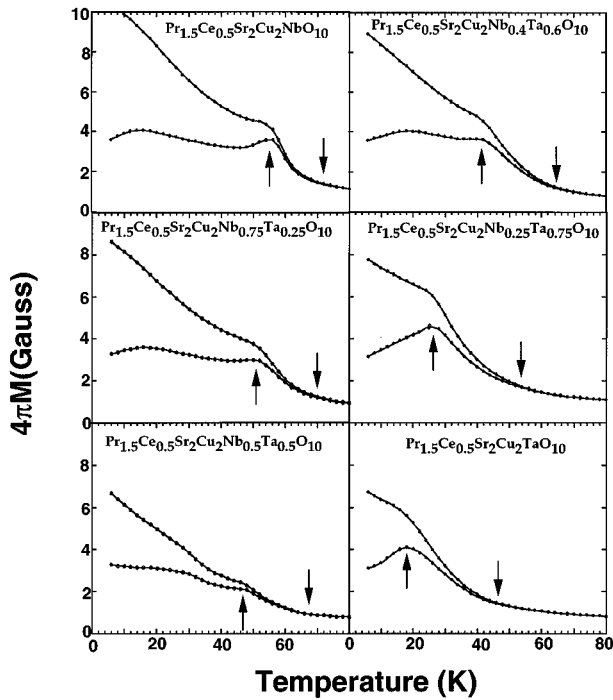


FIG. 2. Zero-field-cooled and field-cooled magnetization spectra taken at 500 Oe for the compounds  $\text{Pr}_{1.5}\text{Ce}_{0.5}\text{Sr}_2\text{Cu}_2\text{Nb}_{1-x}\text{Ta}_x\text{O}_{10}$  ( $x=0.0, 0.25, 0.5, 0.6, 0.75, 1.0$ ). The downward pointing arrow indicates the position of the irreversibility temperature and the upward pointing arrow identifies the temperature of the Cu moment reorientation peak.

downward pointing arrows in Fig. 2, can also be seen to shift towards lower temperatures as one goes across the series of these solid solutions starting from the fully doped Nb end member to the fully doped Ta end member.

The temperature at which the interlayer Cu moment reorientation occurs in these materials under the application of a 500 Oe field, as a function of Nb content, is plotted in Fig. 3. The error bars corresponding to each of the data points shown in this figure are estimated to be  $\pm 1$  K based upon the

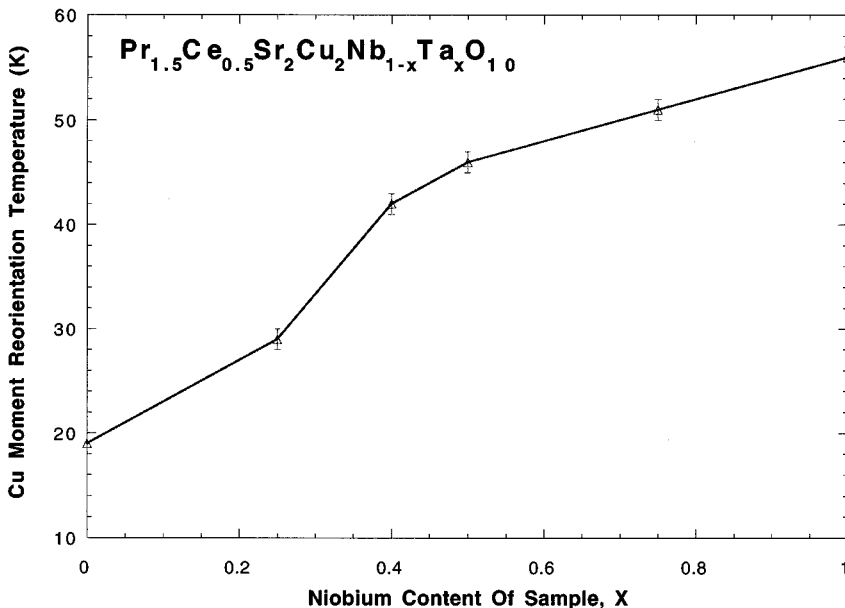


FIG. 3. The Cu spin transition temperature as a function of Nb content in a field of 500 Oe. The vertical error bars in this figure are determined to be  $\pm 1$  K from the slope bisection method used to obtain the data.

slope bisection method that was used to obtain the peak values from the magnetization spectra. The line through these data points is merely a guide for the reader and not a result of any curve fit or theoretical model. The data in Fig. 3 illustrates that the nature of the magnetic interactions driving the Cu spin reordering inherent to these materials is clearly not a linear function of the amount of Ta contained in these compounds.

The effects on the intensity of the magnetic transition peaks due to varying the applied magnetic field for both the Cu spin transition and Pr ion ordering transition in these compounds is shown in Fig. 4 over the temperature range 0–80 K. Experimental results obtained from both of the end members and two of the intermediate compounds are shown. The magnetic spectra were obtained in applied magnetic fields ranging from 50 Oe (circles), 500 Oe (squares), 1 kOe (diamonds), and 5 kOe (cross). In all cases, the net effect that is observed upon increasing the strength of the applied magnetic field is a subsequent reduction in the intensity of the Cu spin transition and enhancement of the lower-temperature Pr magnetic transition. The peak at 15 K has been assigned to an ordering of the Pr sublattice based on an analogy with the  $\text{PrBa}_2\text{Cu}_3\text{O}_7$  and  $\text{PrBa}_2\text{Cu}_2\text{NbO}_8$  materials, which have AF transitions at 17 K and 12 K, respectively.

The behavior of the magnetic peaks as a function of applied field can be simply understood as arising from the convolution of a weak ferromagnetic ordering process riding on a strong paramagnetic background due to the presence of the Pr ions. Upon saturation of the weak ferromagnetic component, under the influence of strong enough applied magnetic fields, the paramagnetic contribution will then dominate. For example, the observed behavior of the magnetic transition peak from the magnetic spectra obtained on the  $\text{Pr}_{1.5}\text{Ce}_{0.5}\text{Sr}_2\text{Cu}_2\text{TaO}_{10}$  sample, namely an apparent 7 K downward shift in the peak position under the application of a 5000 Oe magnetic field, can be readily explained as a result of a superposition of the Cu spin transition which is decreasing in intensity with field and the magnetic ordering peak due to the Pr ions which increases in intensity. As the two

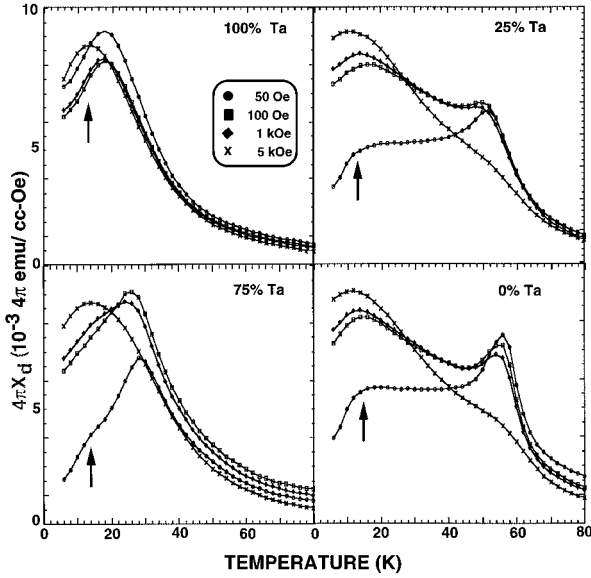


FIG. 4. Magnetization spectra showing the changes in the amplitudes of the magnetic transitions associated with the Cu spin transition and Pr ordering for the  $\text{Pr}_{1.5}\text{Ce}_{0.5}\text{Sr}_2\text{Cu}_2\text{NbO}_{10}$ ,  $\text{Pr}_{1.5}\text{Ce}_{0.5}\text{Sr}_2\text{Cu}_2\text{Nb}_{0.75}\text{Ta}_{0.25}\text{O}_{10}$ ,  $\text{Pr}_{1.5}\text{Ce}_{0.5}\text{Sr}_2\text{Cu}_2\text{Nb}_{0.25}\text{Ta}_{0.75}\text{O}_{10}$ , and  $\text{Pr}_{1.5}\text{Ce}_{0.5}\text{Sr}_2\text{Cu}_2\text{TaO}_{10}$  samples obtained in applied magnetic fields ranging from 50 Oe (circles), 500 Oe (squares), 1 kOe (diamonds), and 5 kOe (crosses). The behavior is explained in the text as the sum of a saturated ferromagnetic component and a dominant paramagnetic background due to the Pr ions. The Pr ion peak is identified by an arrow in the figure.

peaks are in close proximity to one another, the apparent shift in peak position would be greater than in the case where the two magnetic transitions were well separated in temperature as in the case for the fully Nb doped compound. Figure 4 also shows that the ordering peak attributable to the ordering of the Pr ions in these compounds does not change as one goes across the series. This suggests that the presence of Ta or Nb in these compounds does not significantly effect the long-range ordering process of the Pr ions in these crystallo-

TABLE I. Quasi-de Almeida-Thouless fit parameters for the  $\text{Pr}_{1.5}\text{Ce}_{0.5}\text{Sr}_2\text{Cu}_2\text{Nb}_x\text{Ta}_{1-x}\text{O}_{10}$  ( $0 \leq x \leq 1$ ) compounds used in this study.

Compound	$H_0$ (kOe)	$T_{\text{irr}}(0)$	$n$
$\text{Pr}_{1.5}\text{Ce}_{0.5}\text{Sr}_2\text{Cu}_2\text{NbO}_{10}$	23.67	73.39	2.01
$\text{Pr}_{1.5}\text{Ce}_{0.5}\text{Sr}_2\text{Cu}_2\text{Nb}_{0.75}\text{Ta}_{0.25}\text{O}_{10}$	23.81	71.15	2.00
$\text{Pr}_{1.5}\text{Ce}_{0.5}\text{Sr}_2\text{Cu}_2\text{Nb}_{0.5}\text{Ta}_{0.5}\text{O}_{10}$	22.25	65.27	2.03
$\text{Pr}_{1.5}\text{Ce}_{0.5}\text{Sr}_2\text{Cu}_2\text{Nb}_{0.4}\text{Ta}_{0.6}\text{O}_{10}$	21.90	64.09	1.99
$\text{Pr}_{1.5}\text{Ce}_{0.5}\text{Sr}_2\text{Cu}_2\text{Nb}_{0.25}\text{Ta}_{0.75}\text{O}_{10}$	20.04	60.07	1.98
$\text{Pr}_{1.5}\text{Ce}_{0.5}\text{Sr}_2\text{Cu}_2\text{TaO}_{10}$	19.78	49.71	2.00

graphic structures. This peak is identified in the figure with an upward pointing arrow.

The dependence of the irreversibility temperature on the applied magnetic field for all of the samples that were used in this study is illustrated in Fig. 5. The data demonstrate that as the applied field increases, the irreversibility temperature moves towards lower temperatures. This is easily understood by recognizing this as a typical characteristic of weak ferromagnetic behavior. For sufficiently strong magnetic fields, the weak ferromagnetic component becomes totally saturated and there is no longer any path distinction between reversible and irreversible behavior; the two curves will lie exactly on top of each other. The error bars in the determination of the irreversibility temperature in each case is estimated to be  $\pm 1$  K. The curves through the data points are curve fits to a quasi-de Almeida-Thouless relationship of the form<sup>14</sup>

$$T_{\text{irr}}(H_a) = T_{\text{irr}}(0)[1 - (H_a/H_0)]^n, \quad (1)$$

where  $H_a$  is the applied magnetic field,  $H_0$  is the saturation magnetic field, and  $T_{\text{irr}}(0)$  is the irreversibility temperature in the absence of a field. The results of the fitting process are provided in Table I. The regression coefficients were all on the order of 0.99.

From the results of the fitting process, the strength of the applied magnetic field that is required to saturate the weak

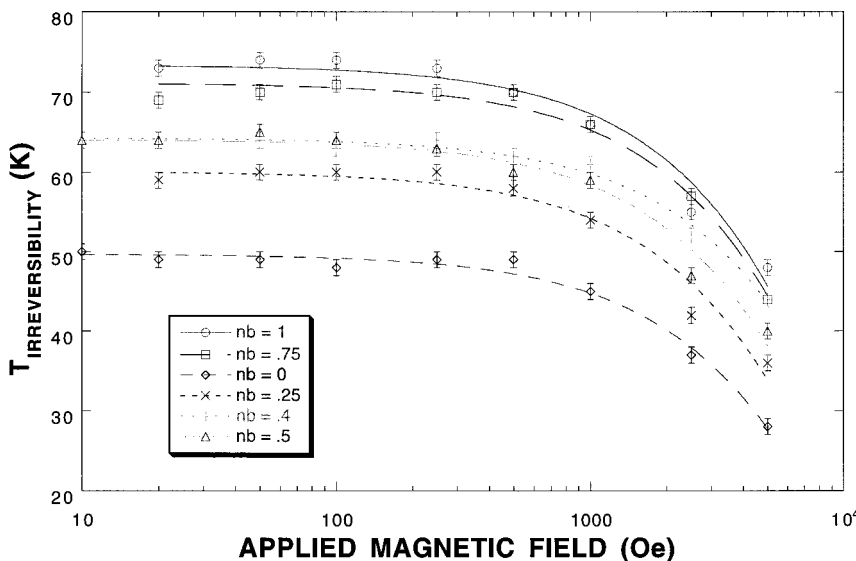


FIG. 5. The irreversibility temperature, measured for the samples used in this study, plotted as a function of the applied magnetic field. The vertical error bars in this figure are determined to be  $\pm 1$  K based upon the slope bisection method used in obtaining the data.

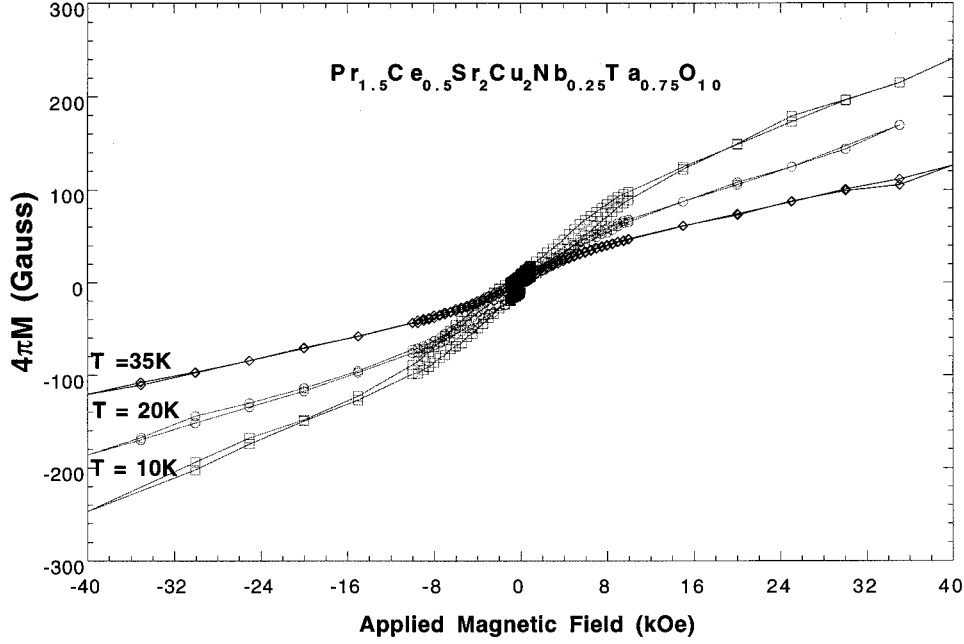


FIG. 6. Isothermal magnetization curves taken at 10, 20, and 35 K for the  $\text{Pr}_{1.5}\text{Ce}_{0.5}\text{Sr}_2\text{Cu}_2\text{Nb}_{0.25}\text{Ta}_{0.75}\text{O}_{10}$  sample obtained in field excursions of  $\pm 40$  kOe. The paramagnetic background at the higher fields due to the Pr ions can easily be seen to exhibit a linear behavior with increasing field.

ferromagnetic component in these compounds increases as one sweeps across the series going from the fully doped Ta phase to the fully doped Nb phase. This is consistent with the results previously shown in Fig. 4. This suggests that the magnetic anisotropy linked with the weak ferromagnetic component in these materials is seemingly more pronounced in those compounds having a smaller Ta concentration. As the nature of the magnetocrystalline anisotropy in these types of materials is typically thought to originate from subtle structural distortions,<sup>15-17</sup> i.e., possibly mediated through oxygen bond disorder, Raman experiments could be helpful as a means for identifying local oxygen modes that would arise from defects induced by improper oxygen stoichiometry or displacement, as was previously performed on the  $R_{2-x}\text{Ce}_x\text{CuO}_4$  ( $R=\text{Nd}, \text{Sm}, \text{Eu}, \text{and Gd}$ ) compounds,<sup>17</sup> or potentially identify new superstructures as was demonstrated in the case of  $\text{Y}_2\text{CuO}_4$  and  $\text{Tm}_2\text{CuO}_4$  compounds.<sup>18</sup> Reitveld refinements from x-ray-diffraction measurements taken on the two end members of this series of compounds suggest that while both exhibit rather large anomalous thermal factors in the position of the oxygen, the relative anisotropy is smaller in the fully doped Ta compound than in the fully doped Nb compound.<sup>11</sup>

In an attempt to separate out the contribution of the weak ferromagnetic component to the magnetic susceptibility of these compounds, several hysteresis curves with magnetic-field excursions of  $\pm 50$  kOe were generated for each compound at several different temperatures. An example of one such set of data taken on the  $\text{Pr}_{1.5}\text{Ce}_{0.5}\text{Sr}_2\text{Cu}_2\text{Nb}_{0.25}\text{Ta}_{0.75}\text{O}_{10}$  sample at 10, 20, 35, and 60 K is shown in Fig. 6. Linear curve fits were done on the dc magnetization versus field data over a range of fields high enough to saturate the weak ferromagnetic component for all the samples used in this study. The linear relationship that was used was of the form<sup>11</sup>

$$M_{\text{dc}}(T, H_a > H_0) = M_0(T) + H_a \chi_d(T), \quad (2)$$

where  $H_a$  is the applied external field,  $\chi_d(T) (= \delta M / \delta H)$  is the differential susceptibility,  $H_0$  is the threshold value of the magnetic field for saturating the weak ferromagnetic component, and  $M_0(T)$  is a field independent magnetization due to the saturated Cu ferromagnetism and the action of the internal field  $H_i$  on the Pr ions,

$$M_0(T) = M_{\text{Cu}}(T) + H_i(T) \chi_d(T). \quad (3)$$

For these compounds, neutron diffraction studies<sup>12</sup> have suggested that the Cu moments order antiferromagnetically somewhere between 200 and 300 K. In addition, this study indicates that the weak ferromagnetism saturates in these compounds for applied magnetic-field strengths above 24 kOe. As a result, these values defined the parameter range over which the curve fits were performed.

The differential susceptibility  $\chi_d(T)$  data from 30 to 200 K, obtained from the previous analysis, was in turn modeled as the sum of a temperature independent term,  $\chi_0$ , accounting for the contribution of the conduction electrons and the core electrons, and a Curie-Weiss term,  $C/(T - \theta)$ , contribution from the Pr ions. The results of the curve fits for each sample used in this investigation are provided in Table II below. The Curie constant  $C$  for these compounds is essentially constant across the series and yields an effective moment of  $2.8\mu_B$  for the Pr ions. This is an indication that the long-range interaction of the Pr ions in these compounds is not affected by the substitution of Ta for Nb. The value for the effective moment in these compounds is entirely consistent with estimates previously obtained of the effective moments of Pr ions in compounds with related structures.<sup>19,20</sup>

TABLE II. Results of Curie-Weiss fits of the differential susceptibility  $\chi_d(T)$  for the series of  $\text{Pr}_{1.5}\text{Ce}_{0.5}\text{Sr}_2\text{Cu}_2\text{Nb}_{1-x}\text{Ta}_x\text{O}_{10}$  ( $x=0,0.25,0.5,0.6,0.75,1$ ) compounds. The regression coefficient in each case was  $\sim 0.99$ .

Compound (Nb content)	$4\pi\chi_0$ ( $4\pi$ emu/c.c.)	$C$ [ $\mu_{\text{eff}}$ ] ( $4\pi$ emu K/c.c.)	$\theta$ (K)
0.00	$7.01 \times 10^{-5}$	0.142 [2.82]	-16.9
0.25	$6.74 \times 10^{-5}$	0.141 [2.82]	-16.9
0.40	$6.23 \times 10^{-5}$	0.143 [2.83]	-17.5
0.50	$6.47 \times 10^{-5}$	0.145 [2.84]	-18.7
0.75	$6.91 \times 10^{-5}$	0.147 [2.86]	-19.3
1.00	$6.13 \times 10^{-5}$	0.148 [2.87]	-19.6

It is worthwhile pointing out that it was not possible to back out estimates for the Cu magnetism,  $M_{\text{Cu}}$ , and internal field,  $H_i$ , using methods that have been previously used to estimate these physical parameters as in the case of single crystals of  $\text{Gd}_2\text{CuO}_4$  (Ref. 4) and  $\text{Tb}_2\text{CuO}_4$  (Ref. 15) and ceramic samples of  $R_2\text{CuO}_4$  (Ref. 9) because (1) no common intersection point was found upon extrapolating the high field  $M$  vs  $H$  linear curve fits [Eq. (2)], indicating that the internal fields for these compounds are temperature dependent and (2) no temperature range was found, above the

long-range ordering temperature of the Pr ions out to room temperature, where the field independent magnetization,  $M_0(T)$ , could be reasonably fit to a temperature independent version of Eq. (3). However, it was possible to independently analyze several of the high field  $M$  vs  $H$  profiles, taken at different temperatures, to back out estimates for  $M_{\text{Cu}}$  and  $H_i$  as a function of temperature. The results of this analysis in the case of the two end members is provided in Fig. 7. Similar curves obtained for the other samples under investigation were found to fall between these two bounding curves. This figure demonstrates that above 20 K the internal field for the Nb doped phase is much stronger at any given temperature than in the case of the Ta doped phase. This finding is in agreement with the experimental observation that the Cu moments reorient at a higher temperature in the Nb doped end member than the Ta doped end member indicating that the exchange interactions between the Cu magnetic sublattice with the Pr magnetic sublattice is stronger in the Nb case than the Ta case. Below 20 K the value of the internal field in both curves increases possibly reflecting the long-range ordering of the Pr ions in these materials. In addition, Fig. 7 shows that the value for the saturated Cu moments in the full Ta version of these material systems is much less than that of the full Nb version. Notably, the value for the temperature at which the onset of the magnetic anisotropy occurs in the

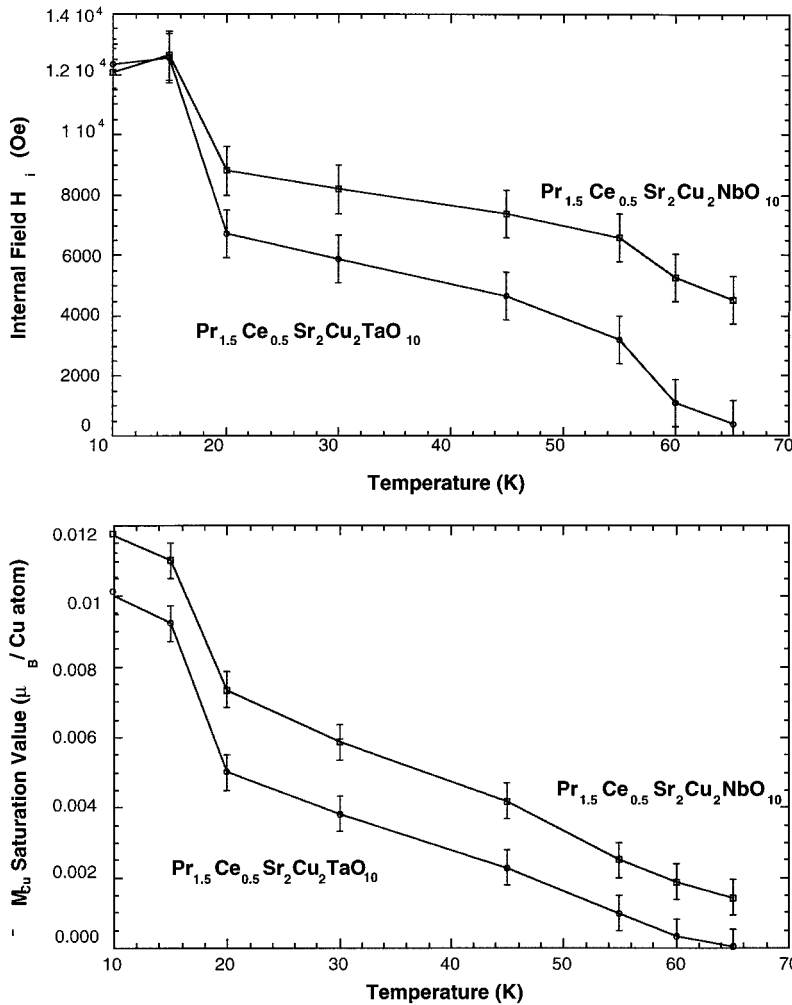


FIG. 7. The results of estimating  $M_{\text{Cu}}$  and  $H_i$  for the  $\text{Pr}_{1.5}\text{Ce}_{0.5}\text{Sr}_2\text{Cu}_2\text{NbO}_{10}$  and  $\text{Pr}_{1.5}\text{Ce}_{0.5}\text{Sr}_2\text{Cu}_2\text{TaO}_{10}$  compounds from  $M$  vs  $H$  profiles. The error bars in estimating the internal field is  $\pm 800$  Oe and for the saturated Cu moment  $\pm 0.0005 \mu_B/\text{Cu}$  atom.

$\text{Pr}_{1.5}\text{Ce}_{0.5}\text{Sr}_2\text{Cu}_2\text{NbO}_{10}$  sample derived from the curve fitting process of Eq. (2) [i.e., when  $M_0(T)$  becomes nonzero] is 130 K, in excellent agreement with the value obtained directly from the neutron diffraction measurements.<sup>12</sup> In the case of the  $\text{Pr}_{1.5}\text{Ce}_{0.5}\text{Sr}_2\text{Cu}_2\text{TaO}_{10}$  sample, the onset temperature is predicted to happen at a somewhat lower temperature, around 110 K. It would prove extremely useful to obtain additional neutron diffraction measurements on the fully doped Ta phase to provide a better understanding of these results.

#### IV. DISCUSSION

In the case of cuprate and nickelate compounds<sup>21</sup> possessing the  $T$  phase crystallographic structure, deviations from a strictly spin-1/2 Heisenberg description of the behavior of the copper and nickel moments have been explained as arising from an antisymmetric exchange interaction resulting in an “out-of-plane” canting of these moments in the AF state, giving rise to a weak ferromagnetic component. The canting is usually made possible because of a slight structural distortion, leading to magnetocrystalline anisotropy, arising from a small rotation of the elongated oxygen octahedra that surround the copper or nickel atoms in these structures.

In the case of cuprate compounds embodying the  $\text{Nd}_2\text{CuO}_4$   $T'$  crystallographic structure the microscopic origin of an inherent “in-plane” weak ferromagnetic component observed in these compounds is not known. However, it has been suggested that the nature of large anomalous anisotropic thermal factors for the oxygen that lie within the square planar  $\text{CuO}_2$  layers observed in several x-ray analysis may result from oxygen displacement within the  $\text{CuO}_2$  planes along the tetragonal direction perpendicular to the Cu-O bond.<sup>15–17</sup> For the heavier rare earths that form  $T'$  solid solutions, such in-plane displacements of the oxygen ions have been estimated to be  $\sim 0.018$  nm. On the other hand, recent neutron diffraction<sup>22</sup> experiments have suggested that an alternative explanation may be that an ordered distortion occurs in these compounds, resulting from the quenching of  $\text{CuO}_4$  square rotations, that would generate a kind of superstructure or symmetry lowering of the unit cell. Such types of superstructures have been confirmed in Raman studies done on  $\text{Y}_2\text{CuO}_4$  and  $\text{Tm}_2\text{CuO}_4$ ,<sup>18</sup> but have not been observed in  $\text{Gd}_2\text{CuO}_4$ .<sup>17</sup>

In either case, the resulting local structural distortion breaks the local tetragonal symmetry of the unit cell and allows for a local canting of the copper moments via a DM interaction of the type  $D_{ij}[S_i \wedge S_j]$  where  $D_{ij}$  is a measure of the coupling strength of the antisymmetric exchange interaction and  $S_i, S_j$  describe the spins of nearest neighbors that are involved in the process. It has been further suggested that the type of disorder associated with these oxygen displacements in these materials might result in a random variation of DM coupling strengths from site to site, introducing frustration into the magnetic system if energy minimization was not achieved simultaneously for all copper pairs. The presence of this random magnetocrystalline anisotropy would most likely favor the formation of microdomains in these compounds. Thus a large number of metastable states could be present that would promote glassy magnetic behavior. Such magnetic characteristics have been reported for the

$\text{Tb}_2\text{CuO}_4$  compound<sup>15</sup> and certainly provides an explanation of the inherent irreversible magnetic behavior observed to happen in all the samples of the series of compounds used in this study. Furthermore, the results of magnetic relaxation measurements performed on the fully doped Ta and Nb end members<sup>11</sup> indicate a logarithmic temporal dependence that is a common feature of magnetic materials like spin glasses or crystal systems with random magnetocrystalline anisotropy. Additional results of dc magnetization measurements obtained on deoxygenated  $\text{Pr}_{1.5}\text{Ce}_{0.5}\text{Sr}_2\text{Cu}_2\text{NbO}_{10}$  samples showed that the two ordering peaks at 13 and 56 K were no longer present in the data, the weak ferromagnetic component was correspondingly weaker, and Curie-Weiss fits to the data still indicated that the Pr ions underwent a long-range AF ordering.<sup>11</sup> Similarly, zero-field-cooled dc magnetization spectra taken on Pr doped samples of  $\text{Eu}_{1.5-x}\text{Pr}_x\text{Ce}_{0.5}\text{Sr}_2\text{Cu}_2\text{NbO}_{10}$  showed that the two peaks were also absent from the data until the concentration of Pr ions into these compounds was greater than 0.6. Interestingly, the temperature at which both magnetic transitions occurred was observed to shift out to higher temperatures as the amount of Pr ions was increased. A detailed description of these experimental findings is currently in preparation. All of these results suggest that a potential factor behind the Cu spin reorientation component of the complex magnetic behavior of these compounds may arise from competition between magnetocrystalline anisotropy and magnetic exchange interactions. This competition could originate because of the different temperature dependence of the internal field, driven by the magnetocrystalline anisotropy, and the temperature dependence of the various rare-earth–rare-earth, rare-earth–transition metal, and transition metal–transition metal exchange processes. The importance of the interrelationship between the magnetocrystalline anisotropy and the magnetic exchange interactions can again be demonstrated by remembering that substitution of nonmagnetic Ce and Th ions in place of the magnetic rare-earth ions in  $R_2\text{CuO}_4$  compounds was shown to significantly depress the temperature at which the weak ferromagnetic behavior occurs in these materials.<sup>10</sup>

A potential picture of the magnetic behavior in these compounds used in this study can be described as (1) from the results of the neutron diffraction measurements the Cu moments order AF below 250 K while the Pr ions follow a Curie-Weiss behavior, (2) below some characteristic temperature, 130 K in the case of the fully doped Nb material, a subtle structural distortion occurs inducing a weak ferromagnetic component via an oxygen mediated antisymmetric exchange interaction between the AF aligned Cu moments, inducing the formation of domains within these compounds; in each domain the Pr ions experiences an internal field that polarizes them in some fashion, (3) when the internal field becomes strong enough, a restructuring of the domains within these materials occurs, that is detected in the dc magnetization and neutron diffraction data as a reorientation of the Cu spins, and (4) below some characteristic temperature the long-range exchange interactions between the Pr ions begin to dominate the effects of the internal fields and the Pr ions order, where presumably the Pr-Cu and Cu-Cu exchange interactions redistribute the various domains in such a way as to minimize the overall energy. Notably, both ferromagnetic and antiferromagnetic short range ordering processes can co-

exist in a random magnetocrystalline anisotropic network, where the nature of the specific magnetic transition depends on the overall average domain structure of the material.<sup>23</sup>

Additional work to get a first order estimate of the energies required for activation of Bloch wall movements of the domains within these compounds, i.e., by potentially doing a careful examination of the coercive fields from hysteresis data, still needs to be performed. Such analysis would help in the process of separating the contributions from magnetocrystalline anisotropy and magnetic exchange interactions to the physical mechanism involved in the apparent lowering of the temperature of the Cu spin transition in going across the series of  $\text{Pr}_{1.5}\text{Ce}_{0.5}\text{Sr}_2\text{Cu}_2\text{Nb}_{1-x}\text{Ta}_x\text{O}_{10}$  ( $0 \leq x \leq 1$ ) compounds. In addition, it may also be possible to derive the temperature profile of the weak ferromagnetic component of the Cu moments from time-logarithmic relaxation measurements performed on these compounds where the coefficient in front of the logarithmic term can be related to the saturation magnetization by a relationship of the form<sup>24</sup>

$$S = 2M_{\text{Cu}}(T)k_B T / \Delta E_a, \quad (4)$$

where  $M_{\text{Cu}}(T)$  is the weak ferromagnetic component,  $k_B$  is Boltzmann's constant, and  $\Delta E_a$  is a flat-topped distribution

of activation energies. The promise of using this method to determine  $M_{\text{Cu}}(T)$  and in turn  $H_i(T)$  using Eq. (3) is currently under investigation for these materials.

For the most part, the evidence of random static distortions (large thermal parameters) have been found only in the  $T'$  compounds that also present weak ferromagnetism, but not in the compounds that can be appropriately doped to promote superconductivity. Consequently, it may be inferred that the reason why superconductivity has not been observed in such systems that exhibit weak ferromagnetic behavior is that the maximum electron doping achievable is not enough to suppress the magnetic order within these systems.<sup>10,25</sup>

#### ACKNOWLEDGMENTS

Work at Lawrence Livermore National Laboratory, UC-Davis, and Northern Carolina A&T was supported in part by the LLNL Research Collaboration Program (RCP) for Historically Black Colleges and Universities under DOE Contract No. W-7405-ENG-48. Part of the work done at UC-Davis was supported by the National Science Foundation under Grant No. DMR-90-21029.

<sup>1</sup>H. B. Radousky, *J. Mater. Res. Soc.* **7**, 1917 (1992).

<sup>2</sup>J. W. Lynn, W-H. Li, H. A. Mook, B. C. Sales, and Z. Fisk, *Phys. Rev. Lett.* **60**, 2781 (1988).

<sup>3</sup>G. W. Crabtree, U. Welp, W. K. Kwok, K. G. Vandervoort, J. Z. Liu, and A. Umezawa, *Physica C* **162-164**, 1299 (1989).

<sup>4</sup>J. D. Thompson, S-W. Cheong, S. E. Brown, Z. Fisk, S. B. Oseroff, M. Tovar, D. C. Vier, and S. Schultz, *Phys. Rev. B* **39**, 6660 (1989).

<sup>5</sup>A. Rouco, X. Obradors, M. Tovar, P. Bordet, D. Chateigner, and J. Chevanas, *Europhys. Lett.* **20**, 651 (1992).

<sup>6</sup>J. Dzyaloshinsky, *J. Phys. Chem. Solids* **4**, 241 (1958).

<sup>7</sup>T. Moriya, *Phys. Rev.* **120**, 91 (1960).

<sup>8</sup>W. Koshibae, Y. Ohta, and S. Maekawa, *Phys. Rev. Lett.* **71**, 467 (1993).

<sup>9</sup>S. B. Oseroff, D. Rao, F. Wright, D. C. Vier, S. Schultz, J. D. Thompson, Z. Fisk, S-W. Cheong, M. F. Hundley, and M. Tovar, *Phys. Rev. B* **41**, 1934 (1990).

<sup>10</sup>A. Butera, A. Caneiro, M. T. Causa, L. B. Steren, R. Zysler, and M. Tovar, *Physica C* **160**, 341 (1989).

<sup>11</sup>T. J. Goodwin, Ph.D. dissertation, U. C. Davis, 1995.

<sup>12</sup>T. J. Goodwin, D. B. Gettman, R. N. Shelton, H. B. Radousky, N. Rosov, J. W. Lynn, and A. Umezawa (unpublished).

<sup>13</sup>T. J. Goodwin, H. B. Radousky, and R. N. Shelton, *Physica C* **204**, 212 (1992).

<sup>14</sup>I. Morgenstern, K. A. Muller, and J. G. Bednorz, *Physica C* **153-155**, 59 (1988).

<sup>15</sup>M. Tovar, X. Obradors, F. Perez, R. J. Duro, J. Rivas, D.

Chateigner, P. Bordet, and J. Chenavas, *Phys. Rev. B* **45**, 4729 (1992).

<sup>16</sup>M. Tovar, X. Obradors, F. Perez, S. B. Oseroff, R. J. Duro, J. Rivas, D. Chateigner, P. Bordet, and J. Chenavas, *J. Appl. Phys.* **70**, 6095 (1991).

<sup>17</sup>M. A. Laguna, M. L. Sanjuan, A. Butera, M. Tovar, Z. Fisk, and P. Canfield, *Phys. Rev. B* **48**, 7565 (1993).

<sup>18</sup>P. Bordet, J. J. Capponi, C. Chailout, D. Chateigner, J. Chenavas, Th. Fournier, J. L. Hodeau, M. Marezio, M. Perroux, G. Thomas, and A. Varela, *Physica C* **185-189**, 539 (1991).

<sup>19</sup>M. Bennahmias, A. F. Bello, D. Back, H. B. Radousky, T. J. Goodwin, P. Klavins, and R. N. Shelton, *Phys. Rev. B* **48**, 6525 (1993).

<sup>20</sup>M. Bennahmias, J. C. O'Brien, H. B. Radousky, T. J. Goodwin, P. Klavins, J. M. Link, C. A. Smith, and R. N. Shelton, *Phys. Rev. B* **46**, 11 986 (1992).

<sup>21</sup>X. Batlle, X. Obradors, and B. Martinez, *Phys. Rev. B* **45**, 2830 (1992).

<sup>22</sup>N. Pyka, N. L. Mitrofanov, P. Bouges, L. Pintschovius, W. Reichart, A. Yu. Rumiantsev, and A. S. Ivanov, *Europhys. Lett.* **18**, 711 (1992).

<sup>23</sup>K. Moorjani and J. M. D. Coey, *Magnetic Glasses* (Elsevier, New York, 1984).

<sup>24</sup>J. I. Arnaud, A. Del Moral, and C. De La Fuente, in *Nanomagnetism*, edited by A. Hernando (Kluwer, Netherlands, 1993).

<sup>25</sup>T. Schultz, R. Smith, A. Fondado, C. Maley, T. Beacom, P. Tinklenberg, J. Gross, C. Saylor, S. B. Oseroff, Z. Fisk, S-W. Cheong, and T. E. Jones, *J. Appl. Phys.* **75**, 6723 (1994).